PAPER

# A parity-time-symmetric optoelectronic oscillator with polarization multiplexed channels

IOP Publishing Journal of Optics
J. Opt. **24** (2022) 055802 (6pp) https://doi.org/10.1088/2040-8986/ac5ecf

# A parity-time-symmetric optoelectronic oscillator with polarization multiplexed channels

**Ege Özgün[1,*], Faruk Uyar[2], Tolga Kartaloglu[2], Ekmel Ozbay[2,3] and Ibrahim Ozdur[4]**

[1] Department of Physics Engineering, Hacettepe University, Beytepe, 06800 Ankara, Turkey
[2] NANOTAM-Nanotechnology Research Center, Bilkent University, 06800 Ankara, Turkey
[3] Department of Physics, Department of Electrical and Electronics Engineering and UNAM-Institute of Materials Science and Nanotechnology, 06800 Ankara, Turkey
[4] Electrical and Electronics Engineering Department, TOBB University of Economics and Technology, 06560 Ankara, Turkey

E-mail: egeozgun@hacettepe.edu.tr

Received 7 January 2022, revised 15 March 2022
Accepted for publication 17 March 2022
Published 5 April 2022

**Abstract**
In this manuscript, we experimentally demonstrate a parity-time-symmetric optoelectronic oscillator (OEO) with polarization multiplexed channels. We obtained a microwave single-mode oscillation at 9.5 GHz with phase noise values of $-116.2$ and $-122.3$ dBc Hz$^{-1}$ at 10 kHz offset frequencies, and side mode suppression values below $-68$ and $-75$ dBc Hz$^{-1}$, by utilizing a 1 km long and 5 km long single mode fiber delay lines, respectively. Our experimental results suggest that parity-time-symmetric OEOs with polarization multiplexed channels are simple and cost-efficient alternatives to their more complex counterparts.

Keywords: optoelectronic oscillators, polarization multiplexing, parity-time symmetry, microwave optics

(Some figures may appear in colour only in the online journal)

## 1. Introduction

Optoelectronic oscillators (OEOs) are devices that are capable of producing stable and low phase noise single microwave modes [1, 2]. The main challenge in OEOs is to maintain single-mode oscillation while further decreasing the phase noise via longer delay lines and high-$Q$ RF band-pass filters. Different schemes such as dual loop [3, 4] and high-$Q$ optical filter [5, 6] were proposed to overcome this problem. Recently, as an alternative approach, the concept of spontaneous symmetry breaking (SSB) from quantum field theories is adopted in an ingenious way for the case of parity time ($\mathcal{PT}$) symmetry-breaking in optical systems [7]. The concept of $\mathcal{PT}$-symmetry was initially introduced within the context of quantum mechanics, which flexes the condition of a quantum mechanical Hamiltonian to be $\mathcal{PT}$-symmetric instead of being Hermitian. Hermiticity guarantees real energy spectra and the unitary evolution of the states which are must conditions to be obeyed within the quantum mechanical systems. However, in late 90s, Bender and Boettcher showed that, those fundamental principles of quantum mechanics can also be satisfied with a $\mathcal{PT}$-symmetric Hamiltonian at least for a certain range of parameters [8, 9]. The concept of pseudo-Hermiticity is then introduced by Mostafazadeh, stating that every Hamiltonian with real spectra are pseudo-Hermitian and that $\mathcal{PT}$-symmetric Hamiltonians belong to that class [10]. The concept of $\mathcal{PT}$-symmetry is then borrowed in the fields of optics and photonics [11–22]. The principal idea behind adopting $\mathcal{PT}$-symmetry in these fields relies on engineering platforms with equal gain/loss which was realized in the aforementioned studies in numerous different ways. Those gave rise to $\mathcal{PT}$-symmetric structures, displaying prominent phenomena including but not

* Author to whom any correspondence should be addressed.

 

limited to, lasing, uni-directional invisibility and anisotropic transmission resonances. $\mathcal{PT}$-symmetry is also studied for the scattering problem with polarization dependence in photonics [23] and for spin-$\frac{1}{2}$ particles in quantum mechanics [24]. The same motivation used in $\mathcal{PT}$-optics studies of equal gain/loss is recently applied to OEOs to overcome the single mode selectivity-long delay line (low phase noise) dilemma [7]. This is achieved via forcing an equal gain/loss $\mathcal{PT}$-symmetric system to go under SSB. Multitude of studies followed the first $\mathcal{PT}$-OEO demonstration: A $\mathcal{PT}$-OEO based on dual wavelength carriers in a single loop configuration [25], tunable $\mathcal{PT}$-OEOs based on dual-parallel Mach–Zehnder modulator [26], based on laser wavelength tuning [27], based on a microdisk resonator [28], based on a microwave photonic filter [29], a polarization-dependent Sagnac loop [30] and non-reciprocal electro-optic modulation [31] are among those.

In this work, we experimentally demonstrate a $\mathcal{PT}$-OEO with polarization multiplexed channels that display all-fiber coupling. The main advantage of utilizing all-fiber coupling is that, only a single photodetector (PD) is sufficient without increasing the complexity, whereas for the RF-coupled $\mathcal{PT}$-OEOs two PDs are required [7, 27]. Previous $\mathcal{PT}$-OEOs that utilize a single PD have complicated schemes, such as implementing dual Mach–Zehnder modulators, dual lasers and micro-disk resonators. [25, 26, 28–31]. Thus, the all-fiber coupled $\mathcal{PT}$-OEO we demonstrate below is both a cost-efficient and a simple alternative.

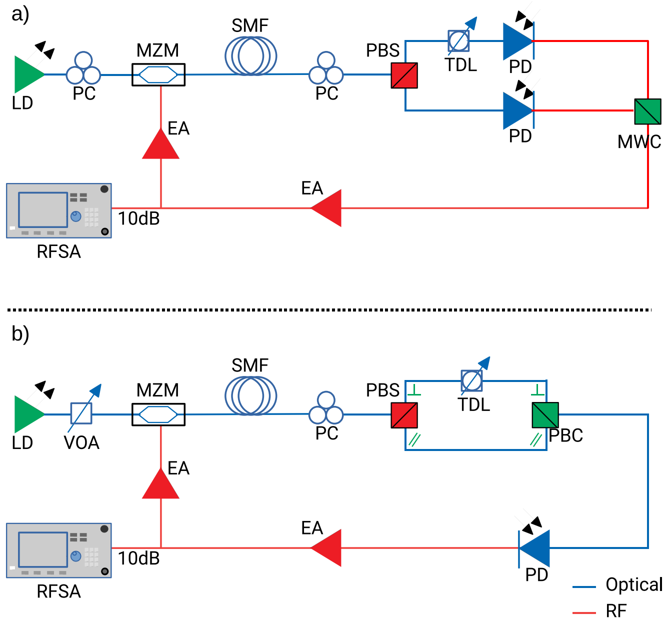


**Figure 1.** (a) Experimental setup used in [7] which utilizes two photodetectors (PD)s for the PT-OEO architecture. (b) Block diagram of the experimental $\mathcal{PT}$-OEO setup based on all-fiber coupling. LD: laser diode, VOA: variable optical attenuator, MZM: Mach–Zehnder modulator, SMF: single mode fiber, PC: polarization controller, PBS: polarization beam splitter, TDL: tunable delay line, PBC: polarization beam combiner, MWC: microwave combiner (RF power combiner), PD: photodetector, EA: electrical amplifier, RFSA: radio frequency spectrum analyzer.

## 2. Experimental setup

The experimental setup used in [7] is given in figure 1(a). As mentioned above, two PDs are utilized for realizing the PT-OEO scheme in that work. In the experimental setup displayed in figure 1(b), the optoelectronic loop starts with a continuous wave light generated from a DFB laser diode (Gooch&Housego EM650). After passing through a variable optical attenuator, it is fed into the Mach Zehnder modulator (Thorlabs LN05S-FC). The modulated signal is sent to a 1 km single mode high-Q optical delay line and the signal is then separated into two channels having equal lengths, with perpendicular polarizations via a polarization beam splitter whose splitting ratio is controlled through a polarization controller. The signal passes through a polarization maintaining (PM) tunable delay line in one channel to balance the phases between two channels. All the fibers and components between the polarization beam splitter and the polarization beam combiner are PM. Afterwards, the two channels are combined at the polarization beam combiner and the signal is converted to RF via the photodetector (Discovery DSC30S). The photodetected signal is then amplified (four ADI HMC-C072-(each providing an average amplification of 6.5 dBm over the range of 7–11 GHz)) and split into two via a 10 dB output coupler. One path is the RF-output for analyses with an RF spectrum analyzer (Keysight PXA N9030B), whereas the other is electrically amplified once more (three ADI HMC-C076-(each providing an average amplification of 8.5 dBm over the range of 6–12 GHz)) and fed back into the modulator to complete the loop. The main difference in our platform from [7] is usage of only a single PD instead of two, via polarization multiplexing. The main advantage of this strategy is two-folds. First, it decreases the cost of the setup considerably, and second, considering the fact that PT-OEO is utilized now in the optical regime, thanks to the low loss of optical fibers, it is easier, as compared to the original architecture, to obtain the PT condition, since for the higher loss due to the cables used in the RF regime a great amount of precision is needed, i.e. even a small amount of difference between length of the loops (i.e. cables) in the RF regime can prevent the realization of the PT condition, where as with the low-loss optical fibers, that much precision is not required. Thus, as given below in section 3, we obtained the same outcome of the original PT-OEO platform for attaining single-mode microwave oscillation without using any filtering device, with only a single PD while enjoying the flexibility brought in by polarization multiplexing which does not require as precise length adjustment of the loops (in our case optical fibers) as in the original design with the cables in RF regime.

It is well-known that the system studied here can be described via the coupled-mode equations [7]:

$$\begin{aligned} i\dot{a}_n &= \omega_n^{(1)} a_n - i g_n a_n - \kappa_n^{12} b_n \\ i\dot{b}_n &= \omega_n^{(2)} b_n + i l_n b_n - \kappa_n^{21} a_n, \end{aligned} \tag{1}$$

where dot denotes time derivative, $a_n$ and $b_n$ are the amplitudes at channels, $\omega_n^{(1)}$ and $\omega_n^{(2)}$ are the frequencies prior to coupling, $g_n$ and $l_n$, are gain and loss amplitudes, respectively and $\kappa_n^{12}$ and $\kappa_n^{21}$ are the coupling coefficient between the channels, for each mode index $n$. For our experimental setup we can take $\omega_n \equiv \omega_n^{(1)} = \omega_n^{(2)}$, ensured by the two loops having equal lengths. For the $\mathcal{PT}$-symmetric configuration, i.e. equal gain and loss ($\gamma_n \equiv g_n = l_n$), the system can be described in the following form:

$$\Omega_n^{(1,2)} = \omega_n \pm \sqrt{\kappa_n^2 - \gamma_n^2}. \tag{2}$$

Here, $\Omega_n^{(1,2)}$ are the eigenfrequencies of our system and $\kappa_n \equiv \kappa_n^{12} = \kappa_n^{21}$ are the coupling coefficients for each mode $n$. When $\gamma_n > \kappa_n$ for any mode $n$, the $\mathcal{PT}$-symmetry becomes broken for that mode, resulting in a single oscillating mode. At this $\mathcal{PT}$-broken regime, the eigenfrequencies are complex conjugate pairs, describing modes at the frequency $\omega_n$ subject to gain and attenuation. The eigenfrequency that is subject to gain gives rise to the oscillating mode.

## 3. Results and discussion

During the experiment, first, all the optical power is directed to one loop using the polarization controller. This gives rise to the NO-$\mathcal{PT}$ configuration as expected and is demonstrated in figure 2(a). Then, we direct the power to both loops this time, giving rise to an equal gain/loss contribution from the two loops. Thus $\mathcal{PT}$-symmetric configuration is achieved, and as $\gamma_n$, controlled via the polarization controller, exceeds the coupling coefficient $\kappa_n$, spontaneous breaking of the $\mathcal{PT}$-symmetry is achieved. As a result, a single mode microwave oscillation at 9.5 GHz is obtained, as plotted in figure 2(b) with a span of 1 MHz and resolution bandwidth (RBW) of 1 kHz. It can be also seen from figure 2(b) that the side-mode suppression ratios of more than 50 dB is measured. This result once more proves that spontaneous breaking of $\mathcal{PT}$-symmetry, is a powerful method for obtaining single mode microwave oscillations without utilizing a high-Q factor filter. It is important to mention that, Mach Zehnder modulator is biased at its quadrature point and the tunable delay line is utilized for balancing the phases of the signals in two loops. The oscillating frequency is determined by $\omega_0$, such that the mode $n = 0$ is the one that experiences $\mathcal{PT}$-symmetry breaking. Thus, the same oscillating frequency can be obtained with delay lines of different length i.e. different $Q$-factors. It is possible to tune $\omega_0$, that was shown for different setups with more complex architecture [26–31].

Figure 3 displays the power spectral density of the single mode microwave signal at 9.5 GHz with a span of 100 MHz and RBW of 100 kHz for the 1 km long single mode delay line. The signal to carrier noise ratio is normalized to 1 Hz bandwidth and calculated to be 130 dBc Hz$^{-1}$. To demonstrate the frequency stability of the $\mathcal{PT}$-OEO, spectrogram is observed for a duration of 100 s and is given in figure 4. The frequency drift is measured to be less than 1 kHz for the duration of 100 s. To investigate the noise characteristics in more detail, we performed phase noise measurements for both 1 km and 5 km delay line cases.

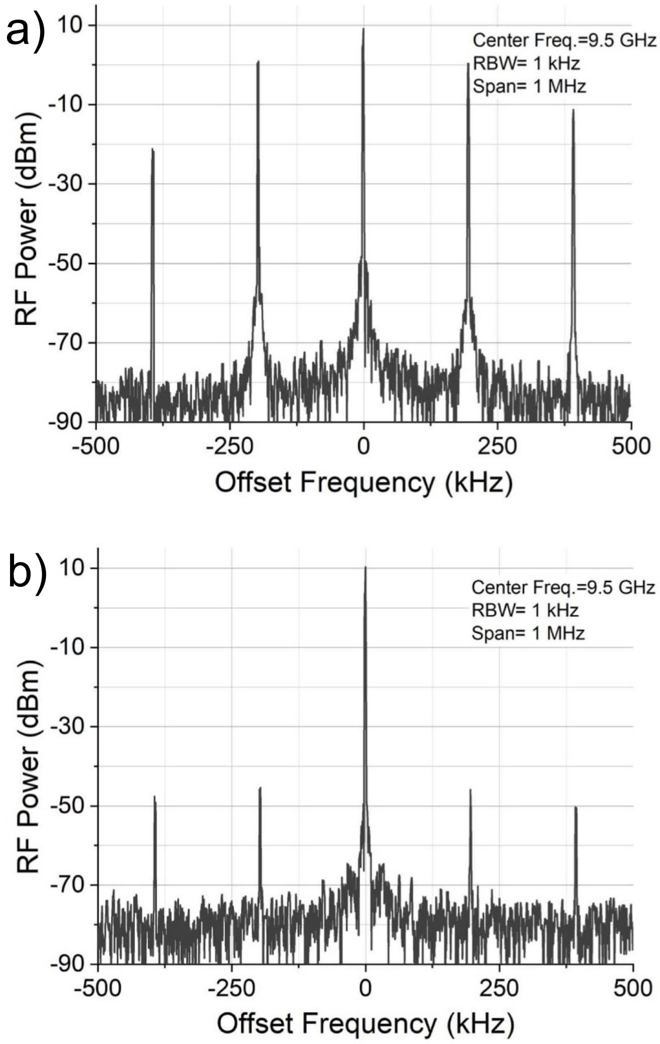


**Figure 2.** (a) One loop (NO-$\mathcal{PT}$) configuration for the 1 km long single mode delay line without oscillation. (b) Single mode oscillation ($\mathcal{PT}$-OEO) at 9.5 GHz for the 1 km long single mode fiber delay line with a span of 1 MHz and RBW of 1 kHz.

Phase noise measurement results for the experimental $\mathcal{PT}$-OEO setup red are displayed in figure 5. At 10 kHz offset, the phase noises of the 1 and 5 km configurations are measured to be $-116.2$ and $-122.3$ dBc Hz$^{-1}$, respectively. For the sake of comparison, the phase noise measurement of the commercial signal generator Keysight PSG E8257D with low phase noise option is also given, together with values obtained from its data sheet [32]. A comparison of the measured values and the ones taken from the data sheet (spline interpolated for a comparison with our measurements) reveals that the measured phase noise values for 1 km and 5 km cases are limited by the noise floor of the measurement device (Keysight PXA N9030B).

A quantitative comparison between the proposed experimental setup herein with different $\mathcal{PT}$-OEO demonstrations would be necessary. Teng *et al* [27] reports a phase noise value of $-116.1$ dBc Hz$^{-1}$ at 10 kHz offset for a 2.6 km long fiber,

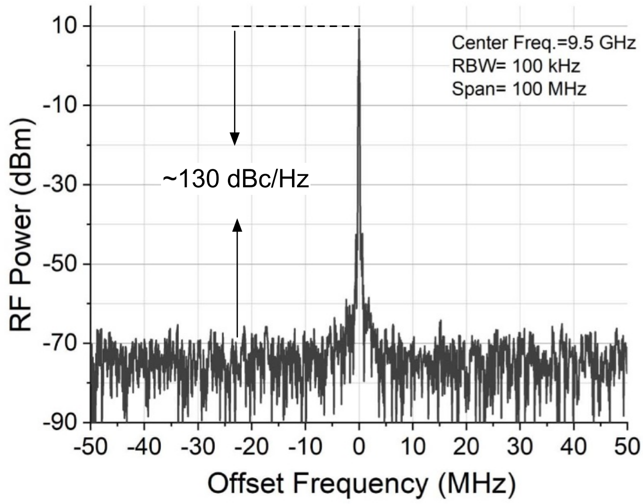


**Figure 3.** Power spectral density of the single mode microwave signal at 9.5 GHz with a span of 100 MHz and RBW of 100 kHz.

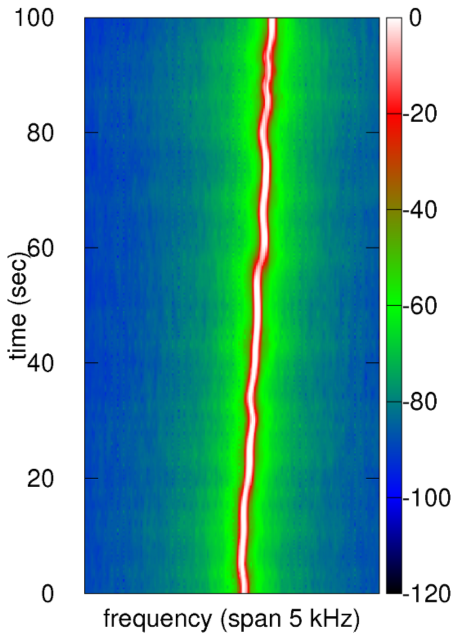


**Figure 4.** Spectogram data given for a span of 5 kHz with a RBW of 50 Hz at the center frequency 9.5 GHz of the oscillating mode for a duration of 100 s.

while [7] reports $-142.5$ dBc $Hz^{-1}$ at the same offset for a setup with 9.166 km long fiber. The proposed platform here demonstrates $-116.2$ and $-122.3$ dBc $Hz^{-1}$ phase noise values at the same offset for 1 and 2 km long fibers respectively. Moreover, the side mode values are measured below $-68$ and $-75$ dBc $Hz^{-1}$ for the setups utilizing 1 and 5 km long fibers respectively for the proposed setup in this manuscript. In [7], sideband suppression value is below $-68.7$ dBc $Hz^{-1}$ for the 9.166 km long loop and for [25] it is below $-66.22$ dBc $Hz^{-1}$ for a 9.1 km long loop. As a result of this comparison, we can safely say that the platform suggested and experimentally demonstrated here is not only on par with the performances of the previously suggested $\mathcal{PT}$-OEOs but for some cases, it is even superior in terms of certain features mentioned above.

It would be needful also to emphasize the comparison between the architecture demonstrated here and the existing ones in the literature once more. The proposed and experimentally demonstrated all-fiber coupled $\mathcal{PT}$-OEO utilizes only a single PD, which simplifies the design in comparison with the RF-coupled $\mathcal{PT}$-OEOs, in which two PDs are required [7, 27]. It is important to emphasize that, while using a single PD by utilizing optical coupling for realizing $\mathcal{PT}$-OEO has no drawbacks, it has a significant advantage: Thanks to the low loss of optical fibers, it is easier, as compared to the original architecture that utilizes RF-coupling, to obtain the $\mathcal{PT}$ condition, since for the higher loss due to the cables used in the RF regime, a great amount of precision is needed, i.e. even a small amount of difference between the length of the

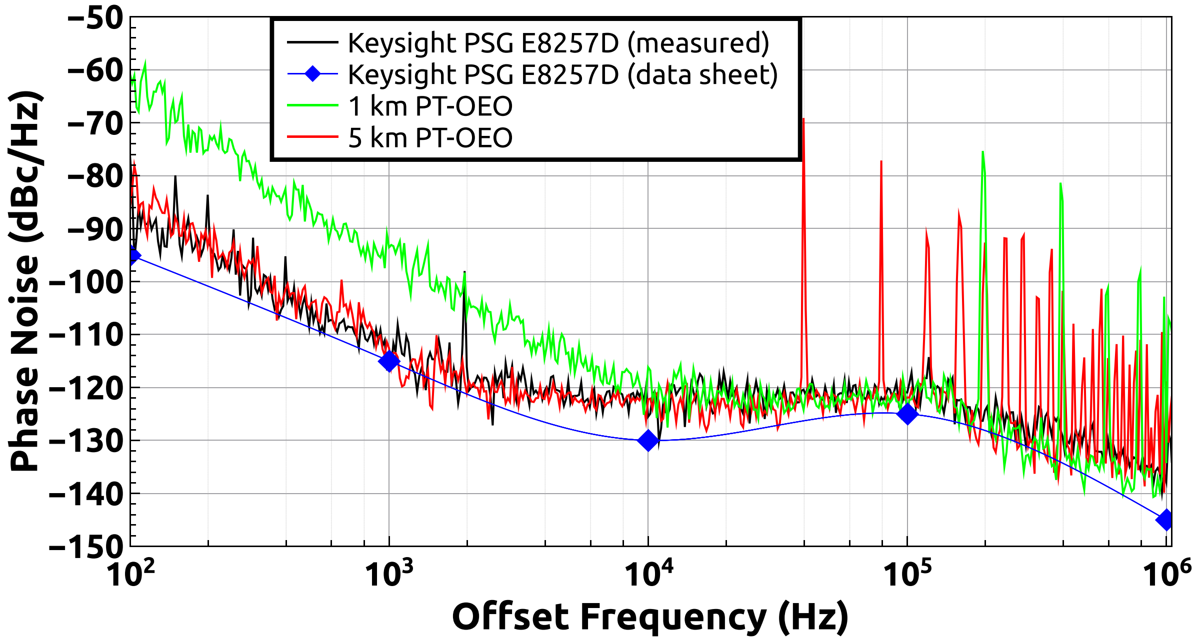


**Figure 5.** Phase noise measurements of $\mathcal{PT}$-OEO with 1 km and 5 km long fibers and of the commercial signal generator (Keysight PSG E8257D), presented together with the data (spline interpolated) taken from the data sheet of the commercial source. The phase noise values at 1 km and 5 km are measured to be $-116.2$ and $-122.3$ dBc Hz$^{-1}$ at 10 kHz offset, respectively. When the measured and given data for the commercial source is compared, it can be seen that our results are limited by the noise floor of the measurement device (Keysight PXA N9030B), thus the actual phase noise values are even lower.

loops (i.e. cables) in the RF regime can prevent the realization of the $\mathcal{PT}$ condition, where as with the low-loss optical fibers, that much precision is not required. Moreover, previous $\mathcal{PT}$-OEOs demonstrated in the literature that utilize a single PD require complicated schemes, such as implementing dual Mach–Zehnder modulators, dual lasers and micro-disk resonators [25, 26, 28–31]. Therefore, the $\mathcal{PT}$-OEO with polarization multiplexed channels demonstrated here has also the advantage of being both a cost-efficient and a simple alternative for the previously demonstrated $\mathcal{PT}$-OEOs.

## 4. Conclusion

To sum up, we have experimentally proposed and demonstrated a $\mathcal{PT}$-OEO with polarization multiplexed channels. Single-mode oscillation is achieved at a microwave frequency of 9.5 GHz. Phase noises of the microwave signals are measured to be $-116.2$ and $-122.3$ dBc Hz$^{-1}$ at 10 kHz offset, and side modes are suppressed with values below $-68$ and $-75$ dBc Hz$^{-1}$ for the 1 km and 5 km long single mode fiber delay lines, respectively. We believe, due to its simplicity and its low-cost, $\mathcal{PT}$-OEOs with polarization multiplexed channels, that display all-fiber coupling, are good candidates for both commercial applications and experimental studies to be conducted on optoelectronic systems.

### Data availability statement

The data that support the findings of this study are available upon reasonable request from the authors.

### Acknowledgment

This work is partially supported by the Turkish Academy of Sciences (TUBA) and the Scientific and Technological Research Council of Turkey (TUBITAK) under the Grant No. 119F265.

### ORCID iD

Ege Özgün https://orcid.org/0000-0001-6186-7087

### References

[1] Yao X S and Maleki L 1996 Optoelectronic oscillator for photonic systems *IEEE J. Quantum Electron.* **32** 1141
[2] Tang J, Hao T, Li W, Domenech D, Baños R, Muñoz P, Zhu N, Capmany J and Li M 2018 Integrated optoelectronic oscillator *Opt. Express* **26** 12257
[3] Yao X S and Maleki L 2000 Multiloop optoelectronic oscillator *IEEE J. Quantum Electron.* **36** 79
[4] Shumakher E and Eisenstein G 2008 A novel multiloop optoelectronic oscillator *IEEE Photonics Technol. Lett.* **20** 1881
[5] Ozdur I, Mandridis D, Hoghooghi N and Delfyett P J 2010 Low noise optically tunable opto-electronic oscillator with Fabry–Perot etalon *J. Lightwave Technol.* **28** 3100
[6] Li W and Yao J 2012 A wideband frequency tunable optoelectronic oscillator incorporating a tunable microwave photonic filter based on phase-modulation to intensity-modulation conversion using a phase-shifted fiber Bragg grating *IEEE Trans. Microw. Theory Tech.* **60** 1735
[7] Zhang J and Yao J 2018 Parity-time–symmetric optoelectronic oscillator *Sci. Adv.* **4** eaar6782

[8] Bender C M and Boettcher S 1998 Real spectra in non-Hermitian Hamiltonians having $\mathcal{PT}$ symmetry *Phys. Rev. Lett.* **80** 5243
[9] Bender C M, Boettcher S and Meisinger P N 1999 PT-symmetric quantum mechanics *J. Math. Phys.* **40** 2201
[10] Mostafazadeh A 2002 Pseudo-Hermiticity versus $\mathcal{PT}$ symmetry: The necessary condition for the reality of the spectrum of a non-Hermitian Hamiltonian *J. Math. Phys.* **43** 205
Mostafazadeh A 2002 Pseudo-Hermiticity versus $\mathcal{PT}$-symmetry. II. A complete characterization of non-Hermitian Hamiltonians with a real spectrum *J. Math. Phys.* **43** 2814
Mostafazadeh A 2002 Pseudo-Hermiticity versus $\mathcal{PT}$-symmetry III: equivalence of pseudo-Hermiticity and the presence of antilinear symmetries *J. Math. Phys.* **43** 3944
[11] El-Ganainy R, Makris K G, Christodoulides D N and Musslimani Z H 2007 Theory of coupled optical PT-symmetric structures *Opt. Lett.* **32** 2632
[12] Musslimani Z, Makris K G, El-Ganainy R and Christodoulides D N 2008 Optical solitons in $\mathcal{PT}$ periodic potentials *Phys. Rev. Lett.* **100** 030402
[13] Makris K G, El-Ganainy R, Christodoulides D N and Musslimani Z H 2008 Beam dynamics in $\mathcal{PT}$ symmetric optical lattices *Phys. Rev. Lett.* **100** 103904
[14] Klaiman S, Günther U and Moiseyev N 2008 Visualization of branch points in $\mathcal{PT}$-symmetric waveguides *Phys. Rev. Lett.* **101** 080402
[15] Guo A, Salamo G J, Duchesne D, Morandotti R, Volatier-Ravat M, Aimez V, Siviloglou G A and Christodoulides D N 2009 Observation of $\mathcal{PT}$-symmetry breaking in complex optical potentials *Phys. Rev. Lett.* **103** 093902
[16] Makris K G, El-Ganainy R, Christodoulides D N and Musslimani Z H $\mathcal{PT}$-symmetric optical lattices *Phys. Rev.* A **81** 063807 2010
[17] Rüter C E, Makris K G, El-Ganainy R, Christodoulides D N, Segev M and Kip D 2010 Observation of parity–time symmetry in optics *Nat. Phys.* **6** 192
[18] Ramezani H, Kottos T, El-Ganainy R and Christodoulides D N 2010 Unidirectional nonlinear $\mathcal{PT}$-symmetric optical structures *Phys. Rev.* A **82** 043803
[19] Feng L, Wong Z J, Ma R-M, Wang Y and Zhang X 2014 Single-mode laser by parity-time symmetry breaking *Science* **346** 972
[20] Zhu X, Feng L, Zhang P, Yin X and Zhang X 2013 One-way invisible cloak using parity-time symmetric transformation optics *Opt. Lett.* **38** 2821
[21] Sounas D L, Fleury R and Alù A 2015 Unidirectional cloaking based on metasurfaces with balanced loss and gain *Phys. Rev. Appl.* **4** 014005
[22] Lin Z, Ramezani H, Eichelkraut T, Kottos T, Cao H and Christodoulides D N 2011 Unidirectional invisibility induced by $\mathcal{PT}$-symmetric periodic structures *Phys. Rev. Lett.* **106** 213901
[23] Özgün E, Serebryannikov A E, Ozbay E and Soukoulis C M 2017 Broadband mixing of $\mathcal{PT}$-symmetric and $\mathcal{PT}$-broken phases in photonic heterostructures with a one-dimensional loss/gain bilayer *Sci. Rep.* **7** 15504
[24] Özgün E, Hakioğlu T and Ozbay E 2020 Scattering of spin-1/2 particles from a $\mathcal{PT}$-symmetric complex potential *Europhys. Lett.* **131** 11001
[25] Li L *et al* 2019 A parity-time-symmetric optoelectronic oscillator based on dual-wavelength carriers in a single spatial optoelectronic loop *2019 Int. Topical Meeting on Microwave Photonics (MWP)* pp 1–4
[26] Ding Q, Wang M, Zhang J, Mu H, Wang C and Fan G 2020 A precisely frequency-tunable parity-time-symmetric optoelectronic oscillator *J. Lightwave Technol.* **38** 6569
[27] Teng C, Zou X, Li P, Xie C, Sun Y, Pan W and Yan L 2020 Fine tunable PT-symmetric optoelectronic oscillator based on laser wavelength tuning *IEEE Photonics Technol. Lett.* **32** 47
[28] Fan Z, Zhang W, Qiu Q and Yao J 2020 Hybrid frequency-tunable parity-time symmetric optoelectronic oscillator *J. Lightwave Technol.* **38** 2127
[29] Li P, Dai Z, Fan Z, Yan L and Yao J 2020 Parity–time-symmetric frequency-tunable optoelectronic oscillator with a single dual-polarization optical loop *Opt. Lett.* **45** 3139
[30] Dai Z, Fan Z, Li P and Yao J 2020 Frequency-tunable parity-time-symmetric optoelectronic oscillator using a polarization-dependent Sagnac loop *J. Lightwave Technol.* **38** 5327
[31] Fan J, Li L, Zhang J, Feng X, Guan B-O and Yao J 2021 A parity-time-symmetric optoelectronic oscillator based on non-reciprocal electro-optic modulation *J. Lightwave Technol.* **39** 2305
[32] Keysight Technologies 2020 *E8257D PSG Microwave Analog Signal Generator* (*Datasheet 5989-0698EN*)